PSFC/JA-20-65

Scattering of Radio Frequency Waves by Density Filaments

Abhay K. Ram[1], K. Hizanidis[2], F. Bairaktaris[2], A. Papadopoulos[2], S.-I. Valvis[2]

[1]Plasma Science and Fusion Center, Massachusetts Institute of Technology, Cambridge, MA
[2]National Technical University of Athens, Athens, Greece

September 2020

Plasma Science and Fusion Center
Massachusetts Institute of Technology
Cambridge MA 02139 USA

AKR is supported by DoE Grant Numbers DE-FG02-91ER-54109 and DE-SC0018090.

Submitted to *Radiation Effects and Defects in Solids*

Scattering of Radio Frequency Waves by Density Filaments

Abhay K. Ram[1], K. Hizanidis[2], F. Bairaktaris[2], A. Papadopoulos[2], S.-I. Valvis[2]

[1]*Plasma Science and Fusion Center, Massachusetts Institute of Technology, Cambridge, MA*

[2]*National Technical University of Athens, Athens, Greece*

1 Introduction

The edge region and the scrape-off layer of magnetically confined fusion devices, like tokamaks and stellarators, are replete with turbulent plasma that is a mixture of coherent, blob or filament like, structures [1] and incoherent fluctuations [2]. The variation in the density due to turbulence can be comparable to or greater than the ambient density [2]. As part of an overall effort to optimize the efficiency of operation, radio frequency (RF) waves are commonly used for heating fusion plasmas and, in tokamaks, for generating plasma current needed for confinement and controlling instabilities. The RF waves are excited by antenna structures that are placed near the wall of a fusion device. In order to deliver energy and momentum to charged particles in the core of fusion plasmas, RF waves have to propagate through the turbulent plasma. In present fusion devices, the scrap-off layer and the edge plasma region is of the order of a few centimeters. In reactor type devices, like ITER, this region is expected to be of the order of tens of centimeters. Since the efficiency of operation of a fusion reactor is of prime importance, it is imperative that we understand the effect of turbulence on RF waves. The fluctuations in density lead to changes in the plasma permittivity. As in conventional electrodynamics, the propagation of RF waves through different dielectric media is subject to reflection, refraction, and diffraction. In this paper, we summarize our theoretical and computational studies on the propagation of RF waves through filamentary structures present in the scrape-off layer.

2 Full wave analytical description of RF scattering

In the theoretical construct of the full-wave scattering model, we have considered scattering off either a single spherical blob [3,4] or a single cylindrical filament with its axis aligned along the magnetic field line [5]. For illustrative purposes, we will consider a single filament. We assume that the plasma density inside the filament, and its external surroundings, is homogeneous in space. The ratio of the densities is arbitrary with a step-function variation at the interface of the filament. The magnetic field is uniform everywhere and thermal effects are neglected – the plasma in the scrape-off layer is essentially cold. We disregard temporal variations of the plasma medium as these variations occur over time scales much longer than the transit time, and the oscillation time, of the RF waves.

The propagation of plane RF waves with time variation given by $\exp(-i\omega t)$, where ω is the angular frequency, follows from the Faraday-Ampere equation,

$$\nabla \times \nabla \times \mathbf{E}(\mathbf{r}) - \frac{\omega^2}{c^2} \overleftrightarrow{\mathbf{K}}(\mathbf{r},\omega) \cdot \mathbf{E}(\mathbf{r}) = 0, \tag{1}$$

where $\mathbf{E}(\mathbf{r})$ is the spatially dependent RF electric field vector, c is the speed of light, and $\overleftrightarrow{\mathbf{K}}(\mathbf{r},\omega)$

is the plasma permittivity tensor,

$$\overleftrightarrow{\mathbf{K}}(\mathbf{r},\omega) = \begin{pmatrix} K_\rho & -iK_\phi & 0 \\ iK_\phi & K_\rho & 0 \\ 0 & 0 & K_z \end{pmatrix}. \tag{2}$$

We have assumed that the magnetic field is along the Cartesian z-direction. The matrix elements are [6],

$$\begin{aligned} K_\rho &= 1 - \frac{\omega_{pe}^2}{\omega^2 - \omega_{ce}^2} - \sum_i \frac{\omega_{pi}^2}{\omega^2 - \omega_{ci}^2}, \\ K_\phi &= -\frac{\omega_{ce}}{\omega} \frac{\omega_{pe}^2}{\omega^2 - \omega_{ce}^2} + \sum_i \frac{\omega_{ci}}{\omega} \frac{\omega_{pi}^2}{\omega^2 - \omega_{ci}^2}, \\ K_z &= 1 - \frac{\omega_{pe}^2}{\omega^2} - \sum_i \frac{\omega_{pi}^2}{\omega^2}, \end{aligned} \tag{3}$$

where ω_{pe} (ω_{pi}) and ω_{ce} (ω_{ci}) are the angular electron (ion) plasma frequency and cyclotron frequency, respectively, and the index i represents all the ion species in the plasma. In general, the plasma and cyclotron frequencies can be functions of space through their dependence on the plasma density and the magnetic field, respectively. For analytical tractability, we will ignore any spatial dependence except for the step-function change in density at the interface between the filament and the background plasma. Consequently, $\overleftrightarrow{\mathbf{K}}(\omega)$ is independent of $\mathbf{r}$ but different inside and outside the filament. Then, Eq. (1) is in the form of vector Helmholtz equation and traditional techniques can be used to solve for plasma waves inside and outside the filament [7]. The self-consistent solution is obtained by satisfying the electromagnetic boundary conditions at the surface of the filament. If $\hat{\boldsymbol{\rho}}$ is the outward pointing unit vector at the surface of the filament, the boundary conditions are,

$$\begin{aligned} \hat{\boldsymbol{\rho}} \cdot (\mathbf{D}_I + \mathbf{D}_S)\big|_{\rho=a} &= \hat{\boldsymbol{\rho}} \cdot \mathbf{D}_F\big|_{\rho=a}, \qquad \hat{\boldsymbol{\rho}} \cdot (\mathbf{B}_I + \mathbf{B}_S)\big|_{\rho=a} = \hat{\boldsymbol{\rho}} \cdot \mathbf{B}_F\big|_{\rho=a}, \\ \hat{\boldsymbol{\rho}} \times (\mathbf{E}_I + \mathbf{E}_S)\big|_{\rho=a} &= \hat{\boldsymbol{\rho}} \times \mathbf{B}_F\big|_{\rho=a}, \qquad \hat{\boldsymbol{\rho}} \times (\mathbf{B}_I + \mathbf{B}_S)\big|_{\rho=a} = \hat{\boldsymbol{\rho}} \times \mathbf{B}_F\big|_{\rho=a}, \end{aligned} \tag{4}$$

where the subscripts I, S, and F represent incident and scattered waves in the background plasma, and waves inside the filament, respectively, a is the radius of the filament, $\mathbf{B}$ is the magnetic induction of the electromagnetic fields, and $\mathbf{D} = \epsilon_0 \overleftrightarrow{\mathbf{K}}.\mathbf{E}$ is the electric displacement field. Of the six boundary conditions in Eq. (4), it can be shown that only four are independent [5]. This leads to an interesting consequence – an incoming RF wave can couple part of its power to another cold plasma wave. The cold plasma dispersion relation, for a fixed frequency, yields two normal modes. In experiments, for a given frequency, power is coupled to one particular, desirable RF mode by appropriately phasing the antenna structure. In order to satisfy the boundary conditions (4), the other cold plasma normal mode has to be included. Thus, for example, if an extraordinary wave in the electron cyclotron frequency range is excited by an antenna configuration, the fluctuations can lead some power being transferred to the ordinary wave. Analytical analysis of the full-wave approach shows that filaments can lead to reflection, refraction, diffraction, side-scattering, and shadowing. Associated with these effects is the spatial fragmentation of the Poynting flux due to the propagation of RF waves through the turbulents. Figure (1) shows all these various aspects of full-wave scattering due to a filament. The full-wave results are in contrast to those obtained using the geometrical optics, ray tracing approach, which leads to refraction only.

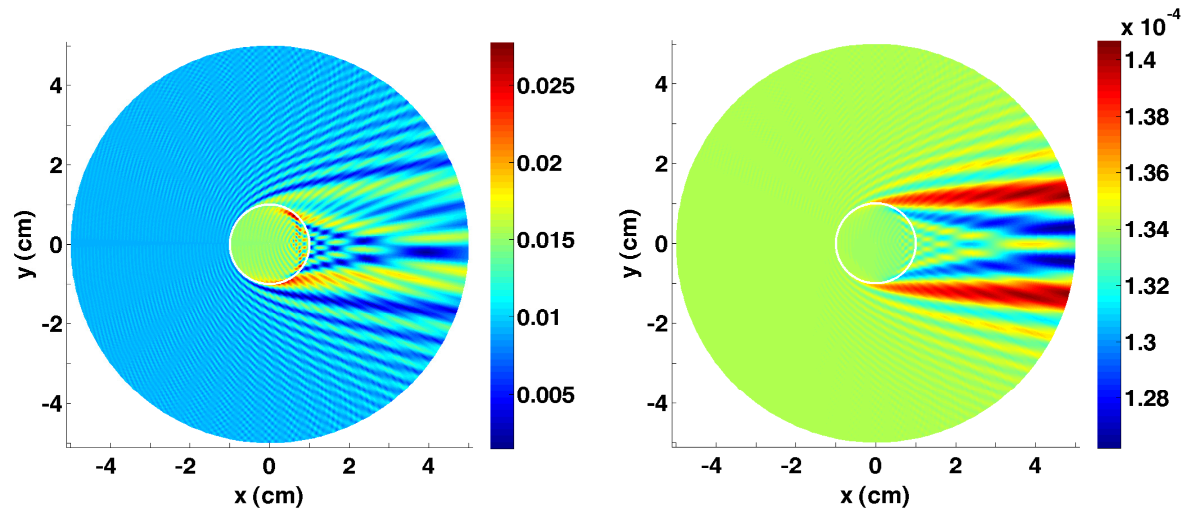

(a) (b)

Figure 1: The scattering of an extraordinary wave in the electron cyclotron range of frequencies by a field aligned filament. The wave is incident from the left and is propagating along the x-axis. The incident wave is elliptically polarized in the $x - y$ plane (normal to the magnetic field along the z-direction). The density inside the filament is 65% greater than the background density. The center of the filament is at $x = y = 0$ and its radius is 1 cm. (a) Contours of $|E_x|$ showing forward scattering of the wave. (b) Contours of $|E_z|$. For the incident wave $E_z = 0$. This figure shows that some of the incident extraordinary wave power has coupled to the ordinary wave.

For a field-aligned filament, the component of the wave vector along the magnetic field, k_z, is preserved during the scattering process; i.e., the incident and scattered waves, and the waves inside the filament have the same k_z. When the axis of the filament is misaligned with respect to the magnetic field, k_z is no longer preserved. As a consequence, the k_z spectrum of the scattered field is broadened [8]. This change in k_z will modify the heating and current profile in the core of a fusion device.

3 Numerical simulations of RF scattering by turbulence

The idealized theoretical model, discussed in the previous section, leads to analytically tractable results. These results serve two purposes. First, they provide a benchmark for any simulation code. Second, the appropriately benchmarked code can be used to determine the range of validity of the analytical results. We developed a simulation code for scattering of RF waves within the COMSOL framework [9, 10]. The code was validated by comparing the numerical results with the analytical results for a step-function discontinuity in density [10]. Subsequently, we extended the simulations to account for a smooth transition from the background plasma to the interior of the filament. We found that, over a broad spatial range of the transition region, the analytical results compared very favorably with the simulations. Finally, we extended the numerical simulations to include multiple filamentary structures of varying dimensions and densities. While these studies are well beyond the capabilities of the analytical model, the essential physics extracted from the single filament theory held true for RF scattering by diverse forms of turbulence [10].

Recently, we have developed a full-wave electromagnetic computational code ScaRF, based on the finite difference frequency domain method [11]. This code was used to study the propagation of a RF plane wave through a spatially modulated, periodic, density interface. Such an interface arises in the edge region due to magnetohydrodynamic instability and/or drift waves. However, the code is general enough to include different varieties of density fluctuations in the edge region. The edge turbulence can be composed of blobs and filaments, and spatially random fluctuations. Our ongoing studies will be making extensive use of ScaRF.

4 Modeling the permittivity of plasmas in the scrape-off layer

The theoretical and computational studies on scattering require a proper description of the plasma permittivity in the turbulent edge region. The tenuous plasma in this region has a broad range of spatial correlations. Electromagnetic homogenization, or "effective medium approximation", is the process of estimating the effective electromagnetic properties of composite materials. We have generalized this approximation, following the Maxwell-Garnett approach, to describe the plasma permittivity in the scrape-off layer [12]. Our formulation is suitably adapted for magnetized plasmas and for RF waves of different frequencies. The advantage of this approach is that we can describe the turbulent plasma as an effective scattering medium with a suitably approximated permittivity. This eliminates the need to have a detailed, microscopic description of the edge plasma. The effective permittivity will be implemented in ScaRF and validated against more descriptive models of the plasma permittivity.

5 Acknowledgments

AKR is supported by DoE Grant Numbers DE-FG02-91ER-54109 and DE-SC0018090.

6 References

[1] S. I. Krasheninnikov, Phys. Lett. A **283**, 368-370 (2001).
[2] S. J. Zweben, J. A. Bodeo, O. Grulke, C. Hidalgo, B. LaBombard, T. J. Maqueda, P. Scarin, and J. L. Terry, Plasma Phys. Controlled Fusion **49**, S1-S23 (2007).
[3] A. K. Ram, K. Hizanidis, and Y. Kominis, Phys. Plasmas **20**, 0566110-1–056110-10 (2013).
[4] A. K. Ram and K. Hizanidis, *Radiation Effects and Defects in Solids: Incorporating Plasma Science and Plasma Technology* (Taylor & Francis, 2013), Vol. 168, pp. 759-775.
[5] A. K. Ram and K. Hizanidis, Phys Plasmas **23**, 022504-1–022504-17 (2016).
[6] T. H. Stix, *Waves in Plasmas* (Springer, New York, 1992), Chaps. 1 and 2.
[7] J. A. Stratton, *Electromagnetic Theory* (McGraw Hill, New York 1941), Chaps. Vi and VII.
[8] S. I. Valvis, A. K. Ram, K. Hizanidis, A. Papadopoulos, A. Zisis, I. G. Tigelis, and E. Glytsis, J. Plasma Physics **84**, 745840604-1–745840604-28 (2018).
[9] See www.comsol.com.
[10] Z. C. Ioannidis, A. K. Ram, K. Hizanidis, and I. G. Tigelis, Phys. Plasmas **24** 102115-1–102115-13 (2017).
[11] A. D. Papadopoulos, E. N. Glytsis, A. K. Ram, S. I. Valvis, P. Papagiannis, K. Hizanidis, and A. Zisis, J. Plasma Physics **85**, 905850309-1–905850309-20 (2019).
[12] F. Bairaktaris, K. Hizanidis, A. K. Ram, P. Papagiannis, C. Tsironis, Y. Kominis, E. Glytsis, O. Chellai, S. Alberti, and I. Furno, J. Plasma Phys. **84**, 745840501-1–745840501-12 (2018).